npg

ORIGINAL ARTICLE

Multiple receptor tyrosine kinases promote the *in vitro* phenotype of metastatic human osteosarcoma cell lines

AN Rettew[1,2], ED Young[3], DC Lev[3], ES Kleinerman[4], FW Abdul-Karim[5], PJ Getty[1] and EM Greenfield[1,2,6]

The survival rate for osteosarcoma patients with localized disease is 70% and only 25% for patients with metastases. Therefore, novel therapeutic and prognostic tools are needed. In this study, extensive screening and validation strategies identified Axl, EphB2, FGFR2, IGF-1R and Ret as specific receptor tyrosine kinases (RTKs) that are activated and promote the *in vitro* phenotype of two genetically different metastatic osteosarcoma cell lines. Initial phosphoproteomic screening identified twelve RTKs that were phosphorylated in 143B and/or LM7 metastatic human osteosarcoma cells. A small interfering RNA (siRNA) screen demonstrated that siRNA pools targeting ten of the twelve RTKS inhibited the *in vitro* phenotype of one or both cell lines. To validate the results, we individually tested the four siRNA duplexes that comprised each of the effective siRNA pools from the initial screen. The pattern of phenotype inhibition replicated the pattern of mRNA knockdown by the individual duplexes for seven of the ten RTKs, indicating the effects are consistent with on-target silencing. Five of those seven RTKs were further validated using independent approaches including neutralizing antibodies (IGF-1R), antisense-mediated knockdown (EphB2, FGFR2, and Ret) or small molecule inhibitors (Axl), indicating that those specific RTKs promote the *in vitro* behavior of metastatic osteosarcoma cell lines and are potential therapeutic targets for osteosarcoma. Immunohistochemistry demonstrated that Axl is frequently activated in osteosarcoma patient biopsy samples, further supporting our screening and validation methods to identify RTKs that may be valuable targets for novel therapies for osteosarcoma patients.

INTRODUCTION

Osteosarcoma, the most common primary bone sarcoma, predominantly affects adolescents in areas of rapid bone growth.[1,2] With the introduction of high-dose, multi-agent chemotherapy regimens in combination with surgical resection in the 1970s, the long-term survival rate increased from 20 to 70% for patients with localized disease.[2–4] Approximately 20% of patients present with overt metastases and 30–40% of patients diagnosed with localized disease go on to develop metastases, with the lungs being the most common sites for metastasis.[2,5] The prognosis for patients with metastases remains poor, with only 20–30% experiencing long-term survival.[6] Therefore, a better understanding of the underlying biology is required to develop improved therapeutic tools.

Unlike cancers with reciprocal chromosomal translocations, osteosarcoma is defined by complex karyotypes with multiple genetic alterations. In addition, there is a large variation of mutations between osteosarcoma patients.[7] Therefore, patient-tailored, targeted therapy might benefit patients that are unresponsive to chemotherapy. Targeted therapy may also be less likely to induce the toxic side effects caused by conventional chemotherapy.[8]

Tyrosine kinases are frequently involved in malignant transformation.[9] The human genome encodes 58 transmembrane receptor tyrosine kinases (RTKs).[10] Most RTKs undergo dimerization and autophosphorylation upon ligand binding, consequently activating downstream signaling cascades.[10,11] Dysregulation or mutations in RTKs can induce aberrant activity and malignant transformation. Tyrosine kinase inhibitors have emerged in the development of targeted anticancer therapy and are available for select RTKs.[12]

Overexpression of several RTKs and their ligands occurs in osteosarcoma, including EGFR, ErbB2, IGF-1R, *met*, NGFR, PDGFR, VEGFR and their ligands.[13–20] Specifically, overexpression of ErbB2, PDGF, PDGFR, VEGF and VEGFR correlates with metastasis and overall poor prognosis in osteosarcoma.[18,19,21–25] However, the underlying role of RTKs in osteosarcoma has not been well characterized and inhibitors have not been approved for treatment.

Because of the variety of mutations between osteosarcoma patients, we used two highly metastatic human osteosarcoma cell lines, 143B and LM7, originally isolated from two different patients.[26,27] The 143B cell line was created from the parental weakly metastatic TE85 cell line by overexpressing oncogenic KRAS.[26] The LM7 cell line was isolated by cycling the parental weakly metastatic Saos2 cells through the lungs of nude mice seven times.[27] To better understand the role of RTKs in

[1]Department of Orthopaedics, Case Western Reserve University, Cleveland, OH, USA; [2]Department of Pathology, Case Western Reserve University, Cleveland, OH, USA; [3]Department of Cancer Biology, The University of Texas MD Anderson Cancer Center, Houston, TX, USA; [4]Division of Pediatrics, The University of Texas MD Anderson Cancer Center, Houston, TX, USA; [5]Department of Anatomic Pathology, Cleveland Clinic Foundation, Cleveland, OH, USA and [6]Case Comprehensive Cancer Center, Case Medical Center, Case Western Reserve University, Cleveland, OH, USA. Correspondence: Dr E Greenfield, Department of Orthopaedics, Case Western Reserve University, 2109 Adelbert Road, Biomedical Research Building, Room 331, Cleveland, OH 44106, USA.
E-mail: emg3@cwru.edu
Received 27 August 2012; accepted 19 September 2012

Figure 2. Functional genomic screening. (**a–e**) siRNA screening of 12 RTKs in LM7 cells after mRNA knockdown by siRNA pools. Knockdown efficiency was assessed by real-time PCR measurements of mRNA levels (mean ± s.e.m. of three PCR well replicates) (**a**) The effect of the siRNA pools on the *in vitro* phenotype was assessed by measuring motility (**b**), colony formation (**c**), invasion (**d**) and cell growth (**e**). (**f–j**) siRNA screening of nine RTKs in 143B cells after mRNA knockdown by siRNA pools. The effect of the siRNA pools on the *in vitro* phenotype was assessed by measuring mRNA expression (**f**), motility (**g**), colony formation (**h**), invasion (**i**) and cell growth (**j**). Results (**b–e** and **g–j**) are compared with cells transfected with the control non-targeting siRNA pool and presented as the percent of control (mean ± s.e.m. of the number of replicates indicated in the methods for each assay). Gray bars represent those siRNA pools that inhibited the indicated assay by ≥35% (below the horizontal line).

Figure 3. IGF-1R contributes to invasion, cell growth, motility and colony formation by the LM7 cell line. (**a–e**) The first validation strategy compared the effects of the siRNA pool to that of the individual duplexes. Knockdown efficiency was assessed by real-time PCR measurements of IGF-1R mRNA levels (mean ± s.e.m. of three PCR well replicates) (**a**). Effects of the siRNAs on *in vitro* phenotypes were assessed by measuring invasion (**b**), cell growth (**c**), motility (**d**) and colony formation (**e**). Results are presented as mean ± s.e.m. of the number of replicates indicated in the Materials and methods for each assay. (**f–j**) The second validation strategy compared the effects of an IGF-1R neutralizing antibody to that of the IGF-1R siRNA pool. Cells were treated for 4 h with the neutralizing antibody. Effects of the antibody and the siRNA pool on IGF-1R activity were assessed by immunoprecipitation with a total IGF-1Rβ antibody followed by western blotting with a phospho-IGF-1R/IR antibody (**f**, top panel) or the total IGF-1Rβ antibody (**f**, middle panel). β-actin was assessed in total cell lysates as a housekeeping protein (**f**, bottom panel). Western blot results are representative of three independent experiments. For expanded views of the blots with protein markers see Supplementary Figure S10. Effects of the neutralizing antibody and the siRNA pool on *in vitro* phenotypes were assessed by measuring invasion (**g**), cell growth (**h**), motility (**i**) and colony formation (**j**). Results are presented as mean ± s.e.m. of three independent experiments.

significantly ($P < 0.03$) inhibited motility and colony formation (Figures 4d–f). Taken together, these results indicate that EphB2 promotes motility and colony formation by LM7 cells.

The FGFR2 siRNA pool and duplexes no. 2 and no. 4 effectively knocked down mRNA expression in LM7 cells, whereas duplexes no. 1 and no. 3 achieved less knockdown (Figure 5a). The pattern of knockdown was similar to the pattern of inhibition for motility and colony formation indicating that these results are consistent with on-target effects (Figures 5b–c). Invasion and cell growth were unaffected in the first-validation experiment (Figures 5d and e), and therefore were not assayed in the second-validation

4

Figure 4. EphB2 contributes to motility and colony formation by the LM7 cell line. (**a**–**c**) The first validation strategy compared the effects of the siRNA pool to that of the individual duplexes. Knockdown efficiency was assessed by real-time PCR measurements of EphB2 mRNA levels (mean ± s.e.m. of three PCR well replicates) (**a**). Effects of the siRNAs on *in vitro* phenotypes were assessed by measuring motility (**b**), and colony formation (**c**). Results are presented as mean ± s.e.m. of the number of replicates indicated in the Materials and methods for each assay. (**d**–**f**) The second validation strategy compared the effects of an antisense LNA/DNA gapmer targeting EphB2 to that of the siRNA pool. Knockdown efficiency by the antisense or siRNA pool was assessed by measuring EphB2 mRNA levels by real-time PCR, comparing levels with cells treated with either the non-targeting antisense LNA/DNA gapmer or the siRNA non-targeting pool (**d**). Effects of the antisense LNA/DNA gapmer and the siRNA pool on *in vitro* phenotypes were assessed by motility (**e**) and colony formation (**f**). Results are presented as mean ± s.e.m. of five independent experiments.

Figure 5. FGFR2 contributes to motility and colony formation by the LM7 cell line. (**a**–**e**) The first validation strategy compared the effects of the siRNA pool with that of the individual duplexes. Knockdown efficiency was assessed by real-time PCR measurements of FGFR2 mRNA levels (mean ± s.e.m. of three PCR well replicates) (**a**). Effects of the siRNAs on *in vitro* phenotypes were assessed by measuring motility (**b**), colony formation (**c**), invasion (**d**) and cell growth (**e**). Results are presented as mean ± s.e.m. of the number of replicates indicated in the Materials and methods for each assay. (**f**–**h**) The second validation strategy compared the effects of an antisense LNA/DNA gapmer targeting FGFR2 with that of the siRNA pool. Knockdown efficiency by the antisense or siRNA pool was assessed by measuring FGFR2 mRNA levels by real-time PCR, comparing levels with cells treated with either the non-targeting antisense LNA/DNA gapmer or the siRNA non-targeting pool (**f**). Effects of the antisense LNA/DNA gapmer and the siRNA pool on *in vitro* phenotypes were assessed by motility (**g**) and colony formation (**h**). Results are presented as mean ± s.e.m. of four independent experiments.

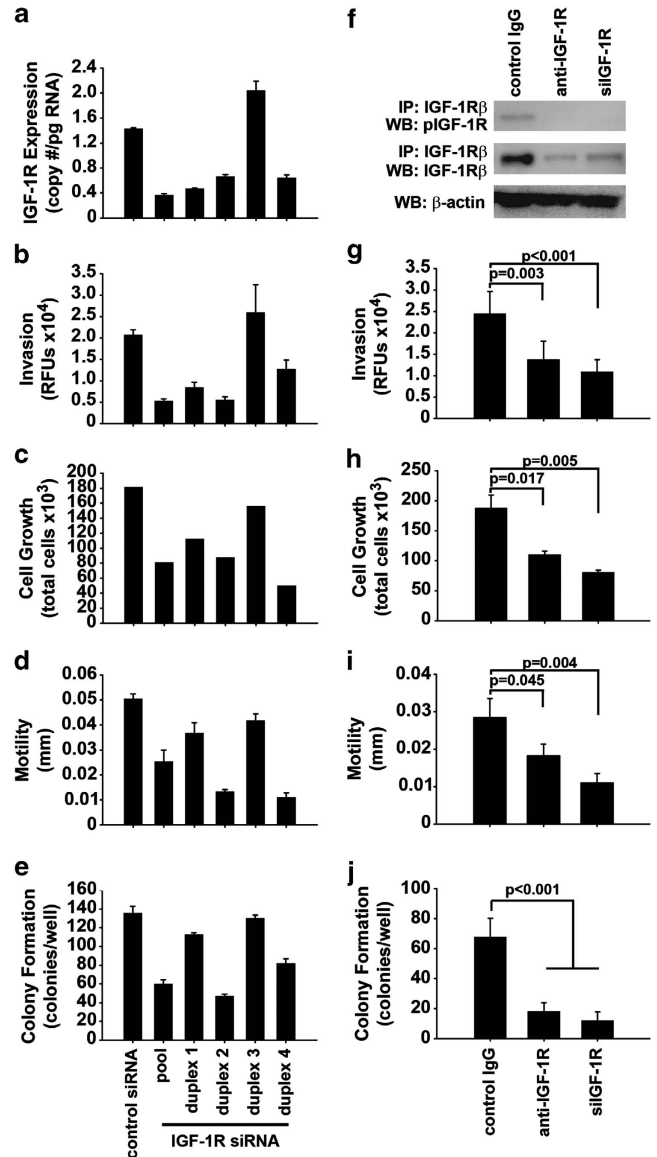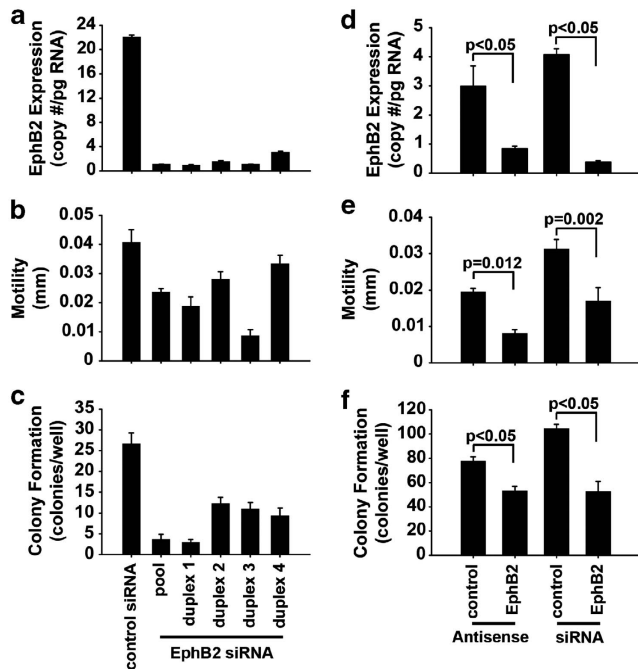experiments, which utilized antisense-mediated knockdown. Both the antisense and siRNA pool effectively knocked down FGFR2 expression and significantly ($P < 0.04$) inhibited motility and colony formation in LM7 cells (Figures 5f–h). These results indicate that FGFR2 promotes motility and colony formation by LM7 cells.

The RET siRNA pool and three of the individual duplexes effectively knocked down mRNA expression in LM7 cells and inhibited motility and colony formation consistent with on-target effects (Figures 6a–c). In contrast, duplex no. 1 had no effect on RET expression but inhibited motility and colony formation, suggesting that its effects were due to off-target silencing (Figures 6d and e). The results for invasion and cell growth were not inhibited and therefore were not assayed in the second-validation experiments, which utilized antisense-mediated knockdown. Both the antisense and siRNA pool effectively knocked down Ret expression and significantly ($P < 0.03$) inhibited motility (Figures 6f and g). Moreover, there was a trend of inhibition of colony formation by both the antisense and the siRNA pool (Figure 6h). Overall, these results indicate that Ret promotes motility and to a lesser extent, colony formation by LM7 cells.

The Axl siRNA pool and each of the four duplexes effectively knocked down Axl expression in 143B cells and inhibited motility,

colony formation and invasion but had no effect on cell growth (Figures 7a–e). The similarity of effects by the individual siRNAs makes it unlikely that the results are due to off-target silencing. The small-molecule inhibitor BGB324 (also known as R428) was used for the second validation. BGB324 was previously shown to be relatively specific for Axl when screened against 133 tyrosine and serine/threonine kinases.[29] BGB324 rapidly reduced Axl phosphorylation in a dose-dependent manner (Figure 7f) and significantly ($P < 0.007$) inhibited motility
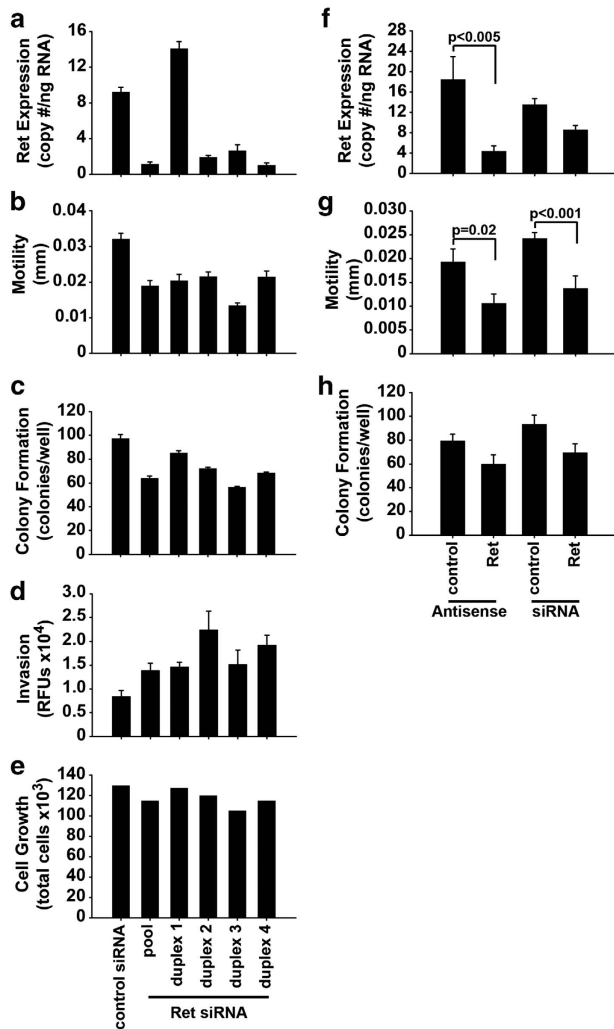
Figure 6. Ret contributes to motility and to a lesser extent, colony formation by the LM7 cell line. (**a**–**e**) The first validation strategy compared the effects of the siRNA pool with that of the individual duplexes. Knockdown efficiency was assessed by real-time PCR measurements of Ret mRNA levels (mean ± s.e.m. of three PCR well replicates) (**a**). Effects of the siRNAs on *in vitro* phenotypes were assessed by measuring motility (**b**), colony formation (**c**), invasion (**d**) and cell growth (**e**). Results are presented as mean ± s.e.m. of the number of replicates indicated in the Materials and methods for each assay. (**f**–**h**) The second validation strategy compared the effects of an antisense LNA/DNA gapmer targeting Ret with that of the siRNA pool. Knockdown efficiency by the antisense or siRNA pool was assessed by measuring Ret mRNA levels by real-time PCR, comparing levels with cells treated with either the non-targeting antisense LNA/DNA gapmer or the siRNA non-targeting pool (**f**). Effects of the antisense LNA/DNA gapmer and the siRNA pool on *in vitro* phenotypes were assessed by motility (**g**) and colony formation (**h**). Results are presented as mean ± s.e.m. of four independent experiments.

and colony formation in a dose-dependent manner (Figures 7g and h). Invasion was only inhibited at the highest concentration of BGB324 (10 μM) (Figure 7i). Furthermore, while 10 μM of BGB324 completely blocked cell growth, 1 μM of BGB324 only inhibited by 15% (Figure 7j). Because of the high concentration of BGB324 needed to inhibit invasion and cell growth, it remains uncertain whether Axl contributes to these phenotypes. Nevertheless, the results indicate that Axl promotes motility and colony formation by 143B cells.
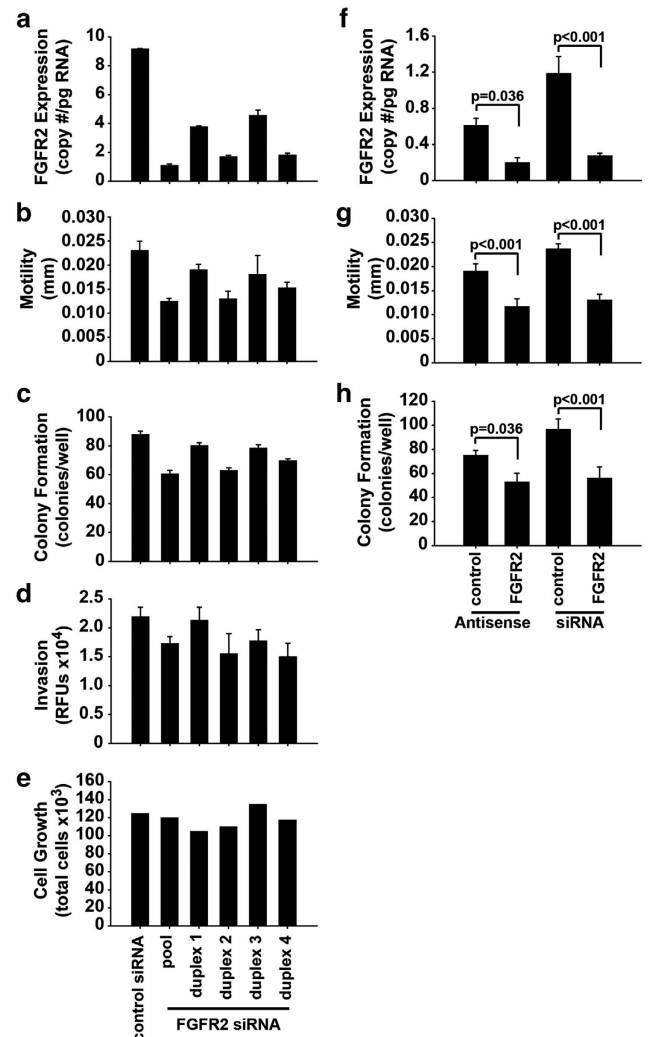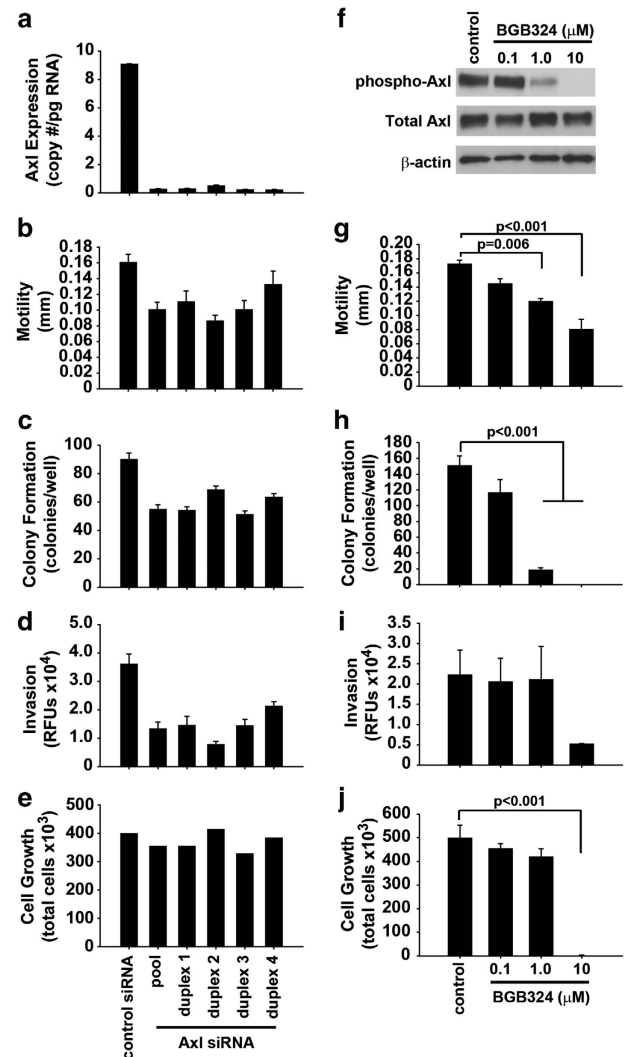
Figure 7. Axl contributes to motility and colony formation by the 143B cell line. (**a**–**e**) The first validation strategy compared the effects of the siRNA pool with that of the individual duplexes. Knockdown efficiency was assessed by real-time PCR measurements of Axl mRNA levels (mean ± s.e.m. of three PCR well replicates) (**a**). Effects of the siRNAs on *in vitro* phenotypes were assessed by measuring motility (**b**), colony formation (**c**), invasion (**d**) and cell growth (**e**). Results are presented as mean ± s.e.m. of the number of replicates indicated in the Materials and methods for each assay. (**f**–**j**) The second validation strategy compared the effects of the Axl small molecule inhibitor, BGB324, with that of the siRNA pool. Cells were treated for 1 h with BGB324 or the control 1% dimethyl sulfoxide. A dose response of Axl activity inhibition by BGB324 was assessed by western blotting with a phospho-Axl antibody (**f**, top panel) or the total Axl antibody (**f**, middle panel). β-actin was assessed as a housekeeping protein (**f**, bottom panel). Western blot results are representative of 10 independent experiments. For expanded views of the blots with protein markers see Supplementary Figure S10. Effects of BGB324 on *in vitro* phenotypes were assessed by measuring motility (**g**), colony formation (**h**), invasion (**i**) and cell growth (**j**). Results are presented as mean ± s.e.m. of three independent experiments.

Immunohistochemistry of patient biopsy samples

Because the above experiments were limited to two osteosarcoma cell lines, we wished to evaluate whether our screening and validation strategies identified targets that are involved in a wider set of patients. Axl activity was chosen for examination in
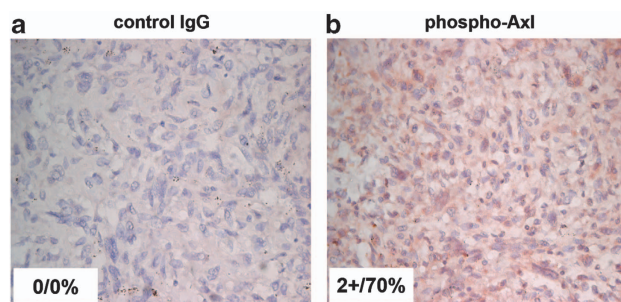
Figure 8. Axl is activated in osteosarcoma patient biopsy samples. (**a** and **b**) Immunohistochemistry was performed on osteosarcoma biopsy samples with an IgG isotype control (**a**) or phospho-Axl (**b**) antibody. Staining was assessed under a light microscope and images were captured at ×400 magnification. The intensity score (left number) and percentage of positive cells (right number) are reported in the inset boxes for each sample.

osteosarcoma patient biopsies as antibodies and protocols for immunostaining of phospho-Axl have already been established.[30] Axl was activated in five of the six patient specimens, with one specimen with weak staining (score = 1+ in 50% of cells) (Supplementary Figure S9) and four specimens with strong staining (score = 3+ in 70–>90% of cells) (Figure 8b and Supplementary Figure S9). Specificity was demonstrated by replacing the primary antibody with non-immune IgG isotype control using the same antigen retrieval and staining conditions as for phospho-Axl (Figure 8a and Supplementary Figure S9). These results indicate that our novel screening and validation strategy identifies targets that may be involved in the underlying biology of the disease in multiple patients.

DISCUSSION

Dysregulation of RTK activity contributes to the progression of many cancers.[9] However, the role of RTKs in the pathogenesis of osteosarcoma has not been well established. In this study, we performed phosphoproteomic screening to identify RTKs that are activated and potentially contribute to signaling within the highly metastatic human LM7 or 143B cells. This also reduced the number of RTKs examined in the functional genomic screen making it feasible to investigate multiple in vitro phenotypes instead of focusing on one high throughput phenotype, such as proliferation, as is common in large-scale screens. In our screen, the siRNAs affected cell growth the least out of the four assays performed, indicating that many important effects would have been missed had we focused solely on cell growth. In support of this methodology, none of the five RTKs that passed both of our validation strategies were identified in a large siRNA screen of kinases that contribute to osteosarcoma cell growth.[31]

Off-target results are the major caveat of siRNA screens. Indeed, the identification of three off-target results in LM7 cells and six in 143B cells supported the importance of the validation strategies, which identified five RTKs for further study. Similar to miRNAs, each siRNA duplex has a seed sequence, nucleotides 2–8 on the guide strand, which directs binding to 3′ untranslated regions of both on-target and off-target genes.[32] BLAST searches performed on the seed sequences of the off-target siRNA duplexes used in our study identified >1800 possible genes for each duplex, making it impractical to determine the genes responsible for the off-target phenotypes.

IGF-1R inhibition reduced all four phenotypes tested in LM7 cells. IGF-1R is one of the few RTKs that has been shown to be important in osteosarcoma.[33] Previously, our lab demonstrated that an IGF-1R small-molecule inhibitor significantly reduced motility and colony formation in LM7 cells.[1] Other studies have

shown that inhibition of IGF-1R reduced proliferation,[34] growth, and invasiveness and induced apoptosis in vitro.[35] IGF-1R neutralizing antibodies inhibited tumor growth in murine xenograft models of osteosarcoma.[36–39] Lung metastasis was inhibited in hypophysectomized mice, which lack IGF-1R signaling.[40] Finally, overexpression of IGF-1R has been reported in osteosarcoma patient samples.[13] This has led to phase I clinical trials using IGF-1R inhibitors in osteosarcoma patients.[41] This strongly supports our screening and validation strategies for identifying RTKs that are important to the in vitro behavior of osteosarcoma.

EphB2 signaling has been implicated in the progression of many cancers including synovial sarcoma[42–44] and colorectal carcinoma.[45] In our study, motility was significantly inhibited in LM7 cells after EphB2 knockdown by either siRNA or antisense. This result is consistent with the finding that Eph receptor signaling is involved in actin cytoskeleton organization thus modulating cell morphology and migration.[42,43] Ephrin expression profiling in osteosarcoma demonstrated that ephrin-A5 and ephrin-B1, ligands for Eph receptors including EphB2, are expressed in osteosarcoma specimens but not in normal bone.[46,47] Our study is the first to demonstrate that EphB2 is important to the in vitro phenotype of osteosarcoma and may be a valuable target for the development of new treatments.

Several genetic alterations of FGFRs have been found in osteosarcoma including single-nucleotide polymorphisms,[48] overexpression[49] and germline amplifications.[50] Two different SMIs targeting FGFRs and VEGF-Rs reduced colony formation or motility by osteoarcoma cell lines.[51,52] FGF2, an FGFR ligand, upregulated migration in an osteosarcoma cell line.[53] Our results indicate that FGFR2 promotes the motility and colony formation of LM7 cells. Taken together with the previous studies, our results indicate that FGFR2 may be important to the underlying biology of osteosarcoma. In contrast, FGFR1 and FGFR4 were not phosphorylated in either cell line and the effects of the FGFR3 siRNA pool in the initial siRNA screen were not reproduced in the validation studies.

Ret inhibition significantly reduced motility in LM7 cells. Our results are consistent with studies demonstrating that Ret contributes to the migration of neuroblastoma, thyroid, pancreatic and non-small cell lung cancer cells.[54–56] While this is the first study to investigate Ret in osteosarcoma, overexpression has been correlated with poor prognosis in liposarcoma.[57]

Our results indicate that Axl promotes the in vitro phenotype of 143B cells. This is consistent with a previous expression profiling study showing that of the genes tested, Axl was upregulated the highest (~40-fold) in metastatic human osteosarcoma cell lines compared with their parental cell lines.[58] However, that study did not determine whether Axl is responsible for the metastatic phenotype of those cell lines.[58] Axl is also overexpressed in liposarcoma[59] and synovial sarcomas.[60] We also demonstrated that BGB324, a selective Axl SMI,[29] reduces Axl phosphorylation, motility and colony formation in a dose-dependent manner. BGB324, which is orally bioavailable and well tolerated in mice, reduces invasion, migration and colony formation in esophageal adenocarcinoma[61] and reduces metastasis in murine models of breast cancer.[29] This supports the investigation of BGB324 as a potential lead compound for targeted therapy in osteosarcoma.

Indicative of the molecular complexity of osteosarcoma, none of the RTKs were validated in both the LM7 and 143B cell lines. Similar to osteosarcoma patients, the 143B and LM7 families of cell lines are genetically different from each other with varying chromosomal aberrations and mutations.[62] It is likely that therapy directed at a single kinase will be unsuccessful at treating all patients and development of multiple therapies targeted to individual patients will be required. In that case, methods to identify potential targets for each patient would be needed. This

could include screening patients for activated RTKs, similar to the anti-phosphoRTK antibody array used in our study.

Due to the extensive screening and validation experiments performed in this study, we focused on two highly metastatic human osteosarcoma cell lines. A recently published study assessed tyrosine phosphoproteins in four other osteosarcoma cell lines.[63] Axl was phosphorylated in all four cell lines, IGF-1R in three, FGFR2 in two and EphB2 in one.[63] Those results, together with the results of our study, indicate that multiple osteosarcoma cell lines with different genetic backgrounds may be dependent on signaling through Axl, IGF-1R, FGFR2 and/or EphB2.

We sought to determine whether Axl is also activated in human patient biopsy samples. Of the six patients examined, one was negative, one scored 1+ and four scored 3+ for phospho-Axl. This indicates that our screening and validation experiments identify targets that may be important in multiple patients. Further analysis of expression levels of the RTKs in human osteosarcoma tissue samples were examined through data mining of online microarray databases. One study available in the Array Express database demonstrated that Axl, EphB2 and FGFR2 mRNAs are upregulated in osteosarcoma samples compared with other cancers (www.ebi.ac.uk/arrayexpress, accession number E-MTAB-62). Oncomine (Compendia Biosciences, Ann Arbor, MI, USA) was also used for the analysis and visualization of one osteosarcoma study showing that FGFR2 mRNA was over-expressed in all five osteosarcoma biopsy samples compared with other sarcomas.[64]

To our knowledge, this is the first study to demonstrate a role for Axl, EphB2, FGFR2 or Ret in the in vitro phenotype of human metastatic osteosarcoma cell lines. Ongoing studies in our laboratory aim to determine whether the RTKs contribute to tumorigenesis and/or metastasis in murine xenograft models of osteosarcoma. Furthermore, the underlying biological mechanisms of RTK activation will be determined to aid development of novel treatments.

MATERIALS AND METHODS

Cell lines and reagents
143B osteosarcoma cells (American Type Culture Collection, Manassa, VA, USA) and LM7 osteosarcoma cells[27] were maintained in minimal essential medium (Hyclone, Logan, UT, USA) with 10% fetal bovine serum (Hyclone), non-essential amino acids (Mediatech, Herndon, VA, USA), 1 mM sodium pyruvate (Invitrogen, Carlsbad, CA, USA), 2 mM L-glutamine (Mediatech) and penicillin-streptomycin (Hyclone). All cells were maintained at 37 °C in 5% CO_2.

The mouse monoclonal IGF-1R neutralizing antibody (MAB391) and mouse IgG$_1$ isotype control antibody (MAB002) were from R&D systems. Rabbit monoclonal antibodies against human Axl (#4566), phospho-Axl (#5724), IGF-1Rβ (#3027), phospho-IGF-1R/IR (#3024), a rabbit polyclonal antibody against β-actin (#4970) and horseradish peroxidase-conjugated anti-rabbit IgG (#7074) were from Cell Signaling Technology (Beverly, MA, USA). BGB324 was kindly provided by Dr Sacha Holland (Rigel Pharmaceuticals Inc, San Francisco, CA, USA).

Phospho-RTK antibody arrays
Cells were washed with phosphate-buffered saline and harvested with NP-40 lysis buffer containing phosphatase and protease inhibitors. The proteome profiler human phosphorylated RTK antibody array (R&D Systems) was performed as recommended by the manufacturer, but with 1 mg of protein lysate per array as preliminary results showed optimal detection with this amount.

Reverse transfection with siRNA or antisense
The four duplexes corresponding to SMARTpool ON-TARGETplus siRNAs were purchased for the indicated RTKs (Dharmacon, Lafayette, CO, USA). In all, 12.5 nM of all four siRNA duplexes was pooled together or 50 nM of each duplex was used alone and incubated for 30 min at room temperature with DharmaFECT Reagent 3 (DF3) in DharmaFECT Cell Culture reagent (DCCR) (Dharmacon). Fifty nanomolar of the ON-TARGETplus Non-targeting siRNA pool was used as the negative control. For antisense-mediated knock-down, 10 nM of the LNA (locked nucleic acid)/DNA gapmer (Exiqon, Woburn, MA, USA) was incubated for 30 min at room temperature with DF3 and DCCR. Ten nanomoles of a non-targeting LNA/DNA gapmer was used as the negative control. Subconfluent cells (75–80%) were harvested and reverse transfected with the siRNA or antisense using 3.0×10^4 cells/cm^2 (143B cells) or 4.0×10^4 cells/cm^2 (LM7 cells) in media without penicillin-streptomycin. Media was changed after 4 h and the cells were incubated for another 44 h before the assays described below.

Motility
Scrape motility assays were performed as previously described.[1] Cells were seeded at a density of 5.0×10^5 cells/cm^2 and incubated overnight to allow formation of a confluent monolayer. Four individual scrapes were created in each monolayer using a 1 ml pipette tip. The media was changed and each scrape was photographed immediately and after 4 h under phase-contrast microscopy. The width of each scrape was measured by ImageJ (NIH, Bethesda, MD, USA) and migration distances were measured by calculating the difference between the scrape width at 0 and 4 h and dividing by 2. Four scrapes were measured per group for each experiment.

Invasion
Invasion was measured using a 96 well Basement Membrane Extract (BME) boyden chamber assay (Trevigen, Gaithersburg, MD) as previously specified.[1] Briefly, 5.0×10^5 cells were resuspended in serum-free media containing 0.1% bovine serum albumin (Proliant Biologicals, Ankeny, IA, USA) and added to the BME-coated upper chamber. Media containing 1% fetal bovine serum was placed in the bottom chamber as a chemo-attractant. After incubation for 24 h, BME-invading cells were incubated with calcein AM and fluorescence measured with the GENiosPro Multimode microplate reader (Tecan, Durham, NC, USA). Six replicates per group were measured for each experiment.

Colony formation
Anchorage-independent colony formation was assayed as previously described.[1] Briefly, a collagen gel containing 1.69 mg/ml rat tail type I collagen (BD Biosciences, Bedford, MA, USA), 0.8× Eagle's minimal essential medium with 5% fetal bovine serum (Hyclone) and 0.75% NaHCO$_3$ (Invitrogen) was added to wells of a 24-well plate and incubated at 37 °C to solidify. Cells were suspended in collagen gel (8.0×10^3 cells/ml) and 160 μl was allowed to solidify over each bottom layer. Gels were covered with 1 ml of 1× minimal essential medium containing 10% fetal bovine serum. Colonies were allowed to form at 37 °C, 5% CO_2 for 2 (143B cells) or 7 days (LM7 cells). Colonies >5 cells were counted using phase-contrast microscopy in triplicate wells per group for each experiment.

Cell growth
Cell growth, defined as the increase in cell number during a 48-h incubation, was measured after plating at a density of 1.0×10^4 cells/cm^2 on a 6-well plate. Cells were harvested after 48 h and one well per group was counted for each experiment.

Quantitative RT–PCR
Total RNA was isolated using the ToTALLY RNA kit (Ambion, Austin, TX, USA). Reverse transcription of total RNA (0.2 μg) was performed using SuperScript II reverse transcriptase (Invitrogen). Quantitative RT–PCR was performed with SYBRgreen PCR Master Mix (BioRad, Hercules, CA, USA) and the 7500 Real-Time PCR Systems and Sequence Detection Software (Applied Biosystems, Foster City, CA, USA). Each primer was designed to overlap exon–exon borders using Primer3 software.[65] Primer sequences are listed in a Supplementary Table. Gene expression was analyzed using a standard curve as previously described.[66] Each reaction was performed in triplicate.

Western blotting and immunoprecipitation
Cells were lysed in 1% Triton X-100 buffer containing protease and phosphatase inhibitors, sonicated briefly and centrifuged for 10 min at 4 °C. Protein concentrations were determined using the BCA Protein Assay Kit (Pierce, Rockford, IL, USA). For western blotting, protein lysates were separated by SDS–PAGE and transferred to polyvinylidene difluoride

membrane. After blocking for 1 h with 5% milk, membranes were incubated with primary antibody overnight at 4 °C. Membranes were then incubated with species-specific horseradish peroxidase-conjugated secondary antibodies. Signals were detected by chemiluminescence (Amersham ECLplus Western blotting detection kit, GE Healthcare, Piscataway Township, NJ, USA). For immunoprecipitation, lysates containing 200 µg of protein were incubated with primary antibodies at 4 °C overnight and then with Protein A Sepharose beads (GE Healthcare) for 60 min at 4 °C. Immunoprecipitates were washed, resuspended in SDS sample buffer with dithiothreitol (DTT) and boiled for western blot analysis.

Immunohistochemistry

Tissue microarray slides were obtained from US Biomax (T262, Rockville, MD, USA) and immunohistochemistry was performed as previously described.[30] Antigen retrieval was performed by incubating in a vegetable steamer for 40 min in Borg Decloaker (BioCare Medical, Concord, CA, USA). The slides were incubated overnight at 4 °C with a rabbit polyclonal anti-phospho-Axl antibody (1:200, R&D systems, #AF2228) or a rabbit IgG non-immune control (Cell Signaling, #3900). The slides were incubated with a biotinylated secondary antibody (BioCare Medical) followed by incubation with horseradish peroxidase-labeled streptavidin. Staining was developed by incubating with diaminobenzidine (Stable DAB, Invitrogen) and counterstaining with Gill's #3 hematoxylin (Fisher Scientific, Pittsburgh, PA, USA). The percentage of positive cells was quantified as well as the intensity (negative = 0, weak = 1+, medium = 2+ or strong staining = 3+) by an experienced bone and tumor pathologist (FWA-K).

Statistical analysis

Data are presented as means ± s.e.m. Statistical analyses were by Two Way ANOVA with Bonferroni post-hoc tests (SigmaStat, San Jose, CA, USA). Data sets that did not pass normality (Kolmogorov–Smirnov test) or equal variance (Levene Median Test) testing (Figures 4d and f) were analyzed non-parametrically by Repeated Measures ANOVA on Ranks with Dunn's post-hoc tests (SigmaStat).

CONFLICT OF INTEREST

The authors declare no conflict of interest.

REFERENCES

1 Messerschmitt PJ, Rettew AN, Brookover RE, Garcia RM, Getty PJ, Greenfield EM. Specific tyrosine kinase inhibitors regulate human osteosarcoma cells in vitro. Clin Orthop Relat Res 2008; 466: 2168–2175.

2 Bielack SS, Kempf-Bielack B, Delling G, Exner GU, Flege S, Helmke K et al. Prognostic factors in high-grade osteosarcoma of the extremities or trunk: an analysis of 1702 patients treated on neoadjuvant cooperative osteosarcoma study group protocols. J Clin Oncol 2002; 20: 776–790.

3 Messerschmitt PJ, Garcia RM, Abdul-Karim FW, Greenfield EM, Getty PJ. Osteosarcoma. J Am Acad Orthop Surg 2009; 17: 515–527.

4 Meyers PA, Schwartz CL, Krailo MD, Healey JH, Bernstein ML, Betcher D et al. Osteosarcoma: the addition of muramyl tripeptide to chemotherapy improves overall survival--a report from the Children's Oncology Group. J Clin Oncol 2008; 26: 633–638.

5 Longhi A, Errani C, DePaolis M, Mercuri M, Bacci G. Primary bone osteosarcoma in the pediatric age: state of the art. Cancer Treat Rev 2006; 32: 423–436.

6 Ferguson WS, Goorin AM. Current treatment of osteosarcoma. Cancer Invest 2001; 19: 292–315.

7 Helman L, Meltzer P. Mechanisms of sarcoma development. Nat Rev Cancer 2003; 3: 685–694.

8 Baselga J. Targeting tyrosine kinases in cancer: the second wave. Science 2006; 312: 1175–1178.

9 Krause DS, Van Etten RA. Tyrosine kinases as targets for cancer therapy. N Engl J Med 2005; 353: 172–187.

10 Hubbard SR, Till JH. Protein tyrosine kinase structure and function. Annu Rev Biochem 2000; 69: 373–398.

11 Chong PK, Lee H, Kong JW, Loh MC, Wong CH, Lim YP. Phosphoproteomics, oncogenic signaling and cancer research. Proteomics 2008; 8: 4370–4382.

12 Fabbro D, Cowan-Jacob SW, Mobitz H, Martiny-Baron G. Targeting cancer with small-molecular-weight kinase inhibitors. Methods Mol Biol 2012; 795: 1–34.

13 Burrow S, Andrulis IL, Pollak M, Bell RS. Expression of insulin-like growth factor receptor, IGF-1, and IGF-2 in primary and metastatic osteosarcoma. J Surg Oncol 1998; 69: 21–27.

14 Benini S, Baldini N, Manara MC, Chano T, Serra M, Rizzi S et al. Redundancy of autocrine loops in human osteosarcoma cells. Int J Cancer 1999; 80: 581–588.

15 Hughes DP, Thomas DG, Giordano TJ, McDonagh KT, Baker LH. Essential erbB family phosphorylation in osteosarcoma as a target for CI-1033 inhibition. Pediatr Blood Cancer 2006; 46: 614–623.

16 Charity RM, Foukas AF, Deshmukh NS, Grimer RJ. Vascular endothelial growth factor expression in osteosarcoma. Clin Orthop Relat Res 2006; 448: 193–198.

17 Ferracini R, Di Renzo MF, Scotlandi K, Baldini N, Olivero M, Lollini P et al. The Met/HGF receptor is over-expressed in human osteosarcomas and is activated by either a paracrine or an autocrine circuit. Oncogene 1995; 10: 739–749.

18 Lee YH, Tokunaga T, Oshika Y, Suto R, Yanagisawa M, Tomisawa M et al. Cell-retained isoforms of vascular endothelial growth factor (VEGF) are correlated with poor prognosis in osteosarcoma. Eur J Cancer 1999; 35: 1089–1093.

19 Sulzbacher I, Birner P, Trieb K, Traxler M, Lang S, Chott A. Expression of platelet-derived growth factor-AA is associated with tumor progression in osteosarcoma. Mod Pathol 2003; 16: 66–71.

20 Fukuda T, Ichimura E, Shinozaki T, Sano T, Kashiwabara K, Oyama T et al. Coexpression of HGF and c-Met/HGF receptor in human bone and soft tissue tumors. Pathol Int 1998; 48: 757–762.

21 Gorlick R, Huvos AG, Heller G, Aledo A, Beardsley GP, Healey JH et al. Expression of HER2/erbB-2 correlates with survival in osteosarcoma. J Clin Oncol 1999; 17: 2781–2788.

22 Handa A, Tokunaga T, Tsuchida T, Lee YH, Kijima H, Yamazaki H et al. Neuropilin-2 expression affects the increased vascularization and is a prognostic factor in osteosarcoma. Int J Oncol 2000; 17: 291–295.

23 Kaya M, Wada T, Kawaguchi S, Nagoya S, Yamashita T, Abe Y et al. Increased pretherapeutic serum vascular endothelial growth factor in patients with early clinical relapse of osteosarcoma. Br J Cancer 2002; 86: 864–869.

24 Oda Y, Yamamoto H, Tamiya S, Matsuda S, Tanaka K, Yokoyama R et al. CXCR4 and VEGF expression in the primary site and the metastatic site of human osteosarcoma: analysis within a group of patients, all of whom developed lung metastasis. Mod Pathol 2006; 19: 738–745.

25 Onda M, Matsuda S, Higaki S, Iijima T, Fukushima J, Yokokura A et al. ErbB-2 expression is correlated with poor prognosis for patients with osteosarcoma. Cancer 1996; 77: 71–78.

26 Luu HH, Kang Q, Park JK, Si W, Luo Q, Jiang W et al. An orthotopic model of human osteosarcoma growth and spontaneous pulmonary metastasis. Clin Exp Metastasis 2005; 22: 319–329.

27 Jia SF, Worth LL, Kleinerman ES. A nude mouse model of human osteosarcoma lung metastases for evaluating new therapeutic strategies. Clin Exp Metastasis 1999; 17: 501–506.

28 Hailey J, Maxwell E, Koukouras K, Bishop WR, Pachter JA, Wang Y. Neutralizing anti-insulin-like growth factor receptor 1 antibodies inhibit receptor function and induce receptor degradation in tumor cells. Mol Cancer Ther 2002; 1: 1349–1353.

29 Holland SJ, Pan A, Franci C, Hu Y, Chang B, Li W et al. R428, a selective small molecule inhibitor of Axl kinase, blocks tumor spread and prolongs survival in models of metastatic breast cancer. Cancer Res 2010; 70: 1544–1554.

30 Lusby K, Torres K, Kivlin C, Liu J, Vu T, Young ED et al. Expression of "drugable" tyrosine kinase receptors in MPNST: a potential role for AXL as a novel therapeutic target. Combined Meeting of the Connective Tissue Oncology Society and the Musculoskeletal Tumor Society;. Chicago, 2011, p 132.

31 Yamaguchi U, Honda K, Satow R, Kobayashi E, Nakayama R, Ichikawa H et al. Functional genome screen for therapeutic targets of osteosarcoma. Cancer Sci 2009; 100: 2268–2274.

32 Jackson AL, Burchard J, Schelter J, Chau BN, Cleary M, Lim L et al. Widespread siRNA "off-target" transcript silencing mediated by seed region sequence complementarity. RNA 2006; 12: 1179–1187.

33 Kolb EA, Gorlick R. Development of IGF-IR Inhibitors in Pediatric Sarcomas. Curr Oncol Rep 2009; 11: 307–313.

34 Kappel CC, Velez-Yanguas MC, Hirschfeld S, Helman LJ. Human osteosarcoma cell lines are dependent on insulin-like growth factor I for in vitro growth. Cancer Res 1994; 54: 2803–2807.

35 Wang YH, Wang ZX, Qiu Y, Xiong J, Chen YX, Miao DS et al. Lentivirus-mediated RNAi knockdown of insulin-like growth factor-1 receptor inhibits growth, reduces

invasion, and enhances radiosensitivity in human osteosarcoma cells. *Mol Cell Biochem* 2009; **327**: 257–266.

36 Dong J, Demarest SJ, Sereno A, Tamraz S, Langley E, Doern A *et al*. Combination of two insulin-like growth factor-I receptor inhibitory antibodies targeting distinct epitopes leads to an enhanced antitumor response. *Mol Cancer Ther* 2010; **9**: 2593–2604.

37 Kolb EA, Gorlick R, Houghton PJ, Morton CL, Lock R, Carol H *et al*. Initial testing (stage 1) of a monoclonal antibody (SCH 717454) against the IGF-1 receptor by the pediatric preclinical testing program. *Pediatr Blood Cancer* 2008; **50**: 1190–1197.

38 Kolb EA, Kamara D, Zhang W, Lin J, Hingorani P, Baker L *et al*. R1507, a fully human monoclonal antibody targeting IGF-1R, is effective alone and in combination with rapamycin in inhibiting growth of osteosarcoma xenografts. *Pediatr Blood Cancer* 2010; **55**: 67–75.

39 Wang Y, Lipari P, Wang X, Hailey J, Liang L, Ramos R *et al*. A fully human insulin-like growth factor-I receptor antibody SCH 717454 (Robatumumab) has antitumor activity as a single agent and in combination with cytotoxics in pediatric tumor xenografts. *Mol Cancer Ther* 2010; **9**: 410–418.

40 Pollak M, Sem AW, Richard M, Tetenes E, Bell R. Inhibition of metastatic behavior of murine osteosarcoma by hypophysectomy. *J Natl Cancer Inst* 1992; **84**: 966–971.

41 Bagatell R, Herzog CE, Trippett TM, Grippo JF, Cirrincione-Dall G, Fox E *et al*. Pharmacokinetically guided phase 1 trial of the IGF-1 receptor antagonist RG1507 in children with recurrent or refractory solid tumors. *Clin Cancer Res* 2011; **17**: 611–619.

42 Barco R, Hunt LB, Frump AL, Garcia CB, Benesh A, Caldwell RL *et al*. The synovial sarcoma SYT-SSX2 oncogene remodels the cytoskeleton through activation of the ephrin pathway. *Mol Biol Cell* 2007; **18**: 4003–4012.

43 Pasquale EB. Eph receptors and ephrins in cancer: bidirectional signalling and beyond. *Nat Rev Cancer* 2010; **10**: 165–180.

44 Surawska H, Ma PC, Salgia R. The role of ephrins and Eph receptors in cancer. *Cytokine Growth Factor Rev* 2004; **15**: 419–433.

45 Mao W, Luis E, Ross S, Silva J, Tan C, Crowley C *et al*. EphB2 as a therapeutic antibody drug target for the treatment of colorectal cancer. *Cancer Res* 2004; **64**: 781–788.

46 Fritsche-Guenther R, Noske A, Ungethum U, Kuban RJ, Schlag PM, Tunn PU *et al*. De novo expression of EphA2 in osteosarcoma modulates activation of the mitogenic signalling pathway. *Histopathology* 2010; **57**: 836–850.

47 Varelias A, Koblar SA, Cowled PA, Carter CD, Clayer M. Human osteosarcoma expresses specific ephrin profiles: implications for tumorigenicity and prognosis. *Cancer* 2002; **95**: 862–869.

48 Mirabello L, Yu K, Berndt SI, Burdett L, Wang Z, Chowdhury S *et al*. A comprehensive candidate gene approach identifies genetic variation associated with osteosarcoma. *BMC Cancer* 2011; **11**: 209.

49 Sadikovic B, Yoshimoto M, Chilton-MacNeill S, Thorner P, Squire JA, Zielenska M. Identification of interactive networks of gene expression associated with osteosarcoma oncogenesis by integrated molecular profiling. *Hum Mol Genet* 2009; **18**: 1962–1975.

50 Entz-Werle N, Lavaux T, Metzger N, Stoetzel C, Lasthaus C, Marec P *et al*. Involvement of MET/TWIST/APC combination or the potential role of ossification factors in pediatric high-grade osteosarcoma oncogenesis. *Neoplasia* 2007; **9**: 678–688.

51 Grigoriadis A, Patino-Garcia A, Zandueta C, Kashima T, Weekes D, Lecanda F. The role of FGFR signaling in osteosarcoma progression and metastasis. *16th Annual Meeting of the Connective Tissue Oncology Society*; Paris, France 2010.

52 Glen H, Mason S, Patel H, Macleod K, Brunton VG. E7080, a multi-targeted tyrosine kinase inhibitor suppresses tumor cell migration and invasion. *BMC Cancer* 2011; **11**: 309.

53 Datsis GA, Berdiaki A, Nikitovic D, Mytilineou M, Katonis P, Karamanos NK *et al*. Parathyroid hormone affects the fibroblast growth factor-proteoglycan signaling axis to regulate osteosarcoma cell migration. *FEBS J* 2011; **278**: 3782–3792.

54 Cockburn JG, Richardson DS, Gujral TS, Mulligan LM. RET-mediated cell adhesion and migration require multiple integrin subunits. *J Clin Endocrinol Metab* 2010; **95**: E342–E346.

55 Gil Z, Cavel O, Kelly K, Brader P, Rein A, Gao SP *et al*. Paracrine regulation of pancreatic cancer cell invasion by peripheral nerves. *J Natl Cancer Inst* 2010; **102**: 107–118.

56 Tang JZ, Kong XJ, Kang J, Fielder GC, Steiner M, Perry JK *et al*. Artemin-stimulated progression of human non-small cell lung carcinoma is mediated by BCL2. *Mol Cancer Ther* 2010; **9**: 1697–1708.

57 Cheng H, Dodge J, Mehl E, Liu S, Poulin N, van de Rijn M *et al*. Validation of immature adipogenic status and identification of prognostic biomarkers in myxoid liposarcoma using tissue microarrays. *Hum Pathol* 2009; **40**: 1244–1251.

58 Nakano T, Tani M, Ishibashi Y, Kimura K, Park YB, Imaizumi N *et al*. Biological properties and gene expression associated with metastatic potential of human osteosarcoma. *Clin Exp Metastasis* 2003; **20**: 665–674.

59 Peng T, Zhang P, Liu J, Nguyen T, Bolshakov S, Belousov R *et al*. An experimental model for the study of well-differentiated and dedifferentiated liposarcoma; deregulation of targetable tyrosine kinase receptors. *Lab Invest* 2011; **91**: 392–403.

60 Fernebro J, Francis P, Eden P, Borg A, Panagopoulos I, Mertens F *et al*. Gene expression profiles relate to SS18/SSX fusion type in synovial sarcoma. *Int J Cancer* 2006; **118**: 1165–1172.

61 Alvarez H, Montgomery EA, Karikari C, Canto M, Dunbar KB, Wang JS *et al*. The Axl receptor tyrosine kinase is an adverse prognostic factor and a therapeutic target in esophageal adenocarcinoma. *Cancer Biol Ther* 2010; **10**: 1009–1018.

62 Forbes SA, Bindal N, Bamford S, Cole C, Kok CY, Beare D *et al*. COSMIC: mining complete cancer genomes in the Catalogue of Somatic Mutations in Cancer. *Nucleic Acids Res* 2011; **39**: D945–D950.

63 Bai Y, Li J, Fang B, Edwards A, Zhang G, Bui M *et al*. Phosphoproteomics identifies driver tyrosine kinases in sarcoma cell lines and tumors. *Cancer Res* 2012; **72**: 2501–2511.

64 Baird K, Davis S, Antonescu CR, Harper UL, Walker RL, Chen Y *et al*. Gene expression profiling of human sarcomas: insights into sarcoma biology. *Cancer Res* 2005; **65**: 9226–9235.

65 Rozen S, Skaletsky H. Primer3 on the WWW for general users and for biologist programmers. *Methods Mol Biol* 2000; **132**: 365–386.

66 Dai JC, He P, Chen X, Greenfield EM. TNFalpha and PTH utilize distinct mechanisms to induce IL-6 and RANKL expression with markedly different kinetics. *Bone* 2006; **38**: 509–520.

Supplementary Information accompanies the paper on the Oncogenesis website (http://www.nature.com/oncsis).